ELECTRONIC PROPERTIES
OF SOLIDS

The Special Features of the Hall Effect in GaMnSb Layers Deposited from a Laser Plasma

V. V. Rylkov[a], B. A. Aronzon[a], Yu. A. Danilov[b,c], Yu. N. Drozdov[c], V. P. Lesnikov[b], K. I. Maslakov[a], and V. V. Podol'skiĭ[b]

[a]*Russian Research Center Kurchatov Institute, pl. Akademika Kurchatova 1, Moscow, 123182 Russia*

[b]*Nizhni Novgorod Research Physicotechnical Institute, Nizhni Novgorod State University, pr. Gagarina 23/3, Nizhni Novgorod, 603950 Russia*

[c]*Institute for Physics of Microstructures, Russian Academy of Sciences, Nizhni Novgorod, 603950 Russia*

e-mail: rylkov@imp.kiae.ru; aronzon@imp.kiae.ru

Received September 23, 2004

Abstract—Epitaxial GaMnSb films with Mn contents up to about 10 at. % were obtained by deposition from a laser plasma in vacuum. The growth temperature T_s during deposition was varied from 440 to 200°C, which changed the concentration of holes from 3×10^{19} to 5×10^{20} cm^{-3}, respectively. Structure studies showed that, apart from Mn ions substituting Ga, the GaMnSb layers contained ferromagnetic clusters with Mn and shallow acceptor defects of the Ga_{Sb} type controlled by the T_s value. Unlike single-phase GaMnSb systems studied earlier with negative anomalous Hall effect values and Curie temperatures not exceeding 30 K, the films obtained in this work exhibited a positive anomalous Hall effect, whose hysteresis character manifested itself up to room temperature and was the more substantial the higher the concentration of holes. The unusual behavior of this effect was interpreted in terms of the interaction of charge carriers with ferromagnetic clusters, which was to a substantial extent determined by the presence of Schottky barriers at the boundary between the clusters and the semiconducting matrix; this interaction increased as the concentration of holes grew. The absence of this effect in semiconducting compounds based on III–V Group elements with MnSb or MnAs ferromagnetic clusters was discussed in the literature; we showed that this absence was most likely related to the low hole concentrations in these objects. © 2005 Pleiades Publishing, Inc.

1. INTRODUCTION

Diluted magnetic semiconductors containing magnetic impurities in high concentrations are disordered media, and their properties are therefore determined by disorder to a considerable extent (see review [1]). An enormous number of works have been concerned with disordered media in the presence of only Coulomb interaction, whereas such media under the conditions of joint magnetic and Coulomb interactions remain virtually unstudied, in spite of a fairly strong interest in them [1]. Solid solutions of manganese in semiconducting Group III and V element compounds (in particular, GaMnAs and GaMnSb) [2, 3] are among the diluted magnetic semiconductors that are most intensely developed and studied. The reason for this is comparatively high Curie temperatures of such semiconductors; they can be prepared as heteroepitaxial compositions on single crystalline substrates of the GaAs type, which offers prospects for their integration with instruments traditionally used in semiconducting micro- and optoelectronics [3, 4]. In these materials, Mn is an acceptor impurity; that is, the introduction of Mn into a semiconductor results in the appearance of both local magnetic moments and free holes, which can cause carrier-

induced ferromagnetism [5].[1] It was, however, found [5] that the attainment of high Curie temperatures T_C in these materials ($T_C \geq 77$ K) required the introduction of Mn ions in a semiconducting matrix in concentrations of 10^{20}–10^{21} cm^{-3}, which was much higher than the limit of the equilibrium solubility of Mn. The successful preparation of supersaturated solid solutions of Mn in III–V compound semiconductors was performed using nonequilibrium methods for growing them. The most important among these is low-temperature molecular beam epitaxy at about 250°C [3, 4]. It was shown for the example of $Ga_{1-x}Mn_xAs$ layers [3] that there is an optimum manganese content x (0.05–0.06) at which single-phase monocrystalline films with a zinc blende structure were formed. In these films, Mn atoms substitute Ga at lattice sites and play the role of acceptors. The Curie temperature then increases to about 110 K at a concentration of holes $p = 3.5 \times 10^{20}$ cm^{-3} [3]. Recently, a special technique for decreasing the concentration of donors was used to reach $T_C = 159$ K [6],

---

[1] Direct exchange between Mn ions in these systems is antiferromagnetic in character. The introduction of compensating donors therefore results in the complete suppression of ferromagnetism in them [3].

which was close to the theoretically possible limit [7]. The Curie temperatures of similar layers of single-phase solid solutions of Mn in GaSb, where Mn atoms also predominantly occupy gallium sites and are acceptors, do not exceed 30 K [8]. The T_C value of so-called digital GaSb/Mn alloys (periodic structures) prepared likewise was 80 K [9]. High Curie temperatures can in principle be attained in digital alloys based on supersaturated solid solutions of Mn in III–V compounds (III–Mn–V) (e.g., see [9]). At the same time, at a high manganese content x and/or high growth temperatures, solid solution decay effects are observed and an additional magnetic phase is formed, whose nature is actively discussed at present [9, 10]. Most often, MnAs or MnSb ferromagnetic clusters with a NiAs ($T_C = 318$ and 587 K, respectively [11]) or zinc blende [9] structure play the role of the additional phase.

A key role in studies of the magnetic properties of diluted magnetic semiconductors based on III–Mn–V compounds is played by revealing and studying the special features of the behavior of the anomalous Hall effect, which is, as is well known, proportional to magnetization M for ferromagnetic metals and is related to the influence of spin–orbit coupling on the scattering of spin-polarized electrons [12]. The calculations performed recently [13] show that the anomalous Hall effect in III–Mn–V semiconductors can be caused by corrections to the velocity of carriers related to the so-called Berry phase. The anomalous Hall effect is then also determined by the exchange splitting of spin hole subbands, is proportional to magnetization, and, therefore, the Hall resistance R_H, as in ferromagnetic metals, obeys the equation [3]

$$R_H = \frac{R_0}{d}B + \frac{R_s}{d}M, \qquad (1)$$

where d is the thickness of the diluted magnetic semiconductor layer; R_0 is the constant of the ordinary Hall effect caused by the Lorentz force, which is proportional to the magnetic induction B; and R_s is the anomalous Hall effect constant.

The anomalous Hall effect plays an important role in studies of ferromagnetism in diluted magnetic semiconductors because it is the most direct method for investigating the interaction of charge carriers with the magnetic subsystem. In addition, for thin films, when the influence of a diamagnetic substrate is strong, the anomalous Hall effect can more effectively be used to study magnetic ordering than magnetization measurements [3, 14, 15]. Another and more important reason for using the anomalous Hall effect is the complex character of the magnetic phase that may appear in III–Mn–V materials [9, 10]. For instance, $Ga_{1-x}Mn_xSb$ crystals grown by the Bridgman method ($x = 0.03$–0.14) were reported [16] to exhibit the Curie temperature $T_C \approx 540$ K, which was close to $T_C \approx 587$ K for MnSb clusters; this result was obtained by studying the temperature dependence of magnetization. It is pertinent to mention that the magnetic field dependences of the Hall effect (which were virtually linear) and magnetization presented in [16] were substantially different. In addition, there was no anomalous Hall effect manifestations of MnSb- or MnAs-type ferromagnetic clusters in GaMnSb [8] and GaMnAs [3], respectively, although the contribution of the clusters to magnetization was considerable and observable up to room temperatures. At the same time, the "Curie temperatures" obtained for these systems by measuring the anomalous Hall effect (T_C^*) were noticeably lower than room temperatures ($T_C^* < 10$ K for GaMnSb with MnSb clusters [8]). Accordingly, it is commonly supposed that the T_C^* parameter obtained from anomalous Hall effect measurements for multiphase solutions of Mn in III–V compounds characterizes magnetic ordering of only part of the magnetic subsystem, which nevertheless largely determines the spin polarization of carriers and is of the greatest importance for diluted magnetic semiconductor applications in spintronics. It is therefore no mere chance that, in recent works [6, 8, 14], preference is given to anomalous Hall effect measurements as a method for the observation of spin-polarized carriers and the determination of the magnetic state of III–Mn–V systems at various temperatures. For single-phase solutions, these measurements give the same T_C temperatures as those obtained in magnetization studies [3, 6].

In spite of the important role played by the anomalous Hall effect in III–Mn–V materials, the question of its nature remains open. It was shown recently [17] that the anomalous Hall effect value in GaMnAs is in close agreement with the calculation results [13], and its sign (positive) coincides with the sign of the ordinary Hall effect, in agreement with [13]. The GaMnSb system, however, exhibits a negative Hall effect, whose sign is opposite to that of the ordinary Hall effect [4, 8, 9]. The theory described in [13] does in principle predict a change in the sign of the anomalous Hall effect; this, however, requires that the Fermi energy be close to the top of the Γ_7 band split off because of spin-orbit coupling [18] (in GaSb, $\Delta_0 = 0.75$ eV [19]), which is at variance with the experimental data [8, 9].[2] The question why MnSb- and MnAs-type clusters in the systems under consideration do not influence the anomalous Hall effect also remains open. Indeed, the anomalous Hall effect is observed quite distinctly in diluted ferromagnetic granulated alloys (nanoparticles of ferromagnetic metals in nonmagnetic metallic matrices) and substantially exceeds the ordinary Hall effect component [20]. The Curie temperatures of single-phase

---

[2] It is shown in [18] that the calculations made in [13] are equivalent to the consideration of the anomalous Hall effect in terms of the so-called side-jump model, in which the sign of the anomalous Hall effect should coincide with the sign of carriers. In the skew scattering model, the sign of the anomalous Hall effect can in principle be arbitrary [18].

I, pulse/s
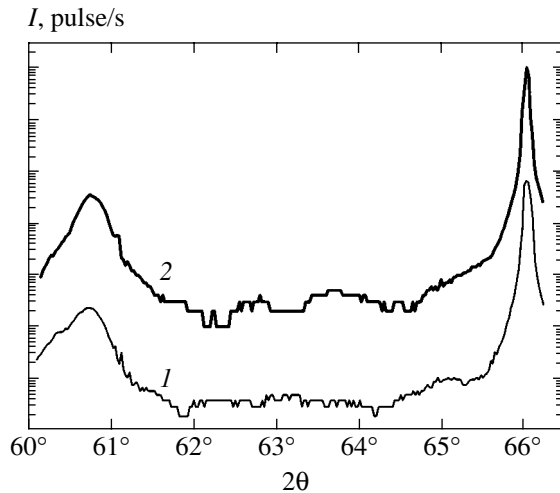
Fig. 1. X-ray diffraction spectra of GaSb/GaAs structures formed by depositing at $T_s = 440°C$: (*1*) undoped and (*2*) doped with manganese. For clarity, the spectra are spaced along the intensity axis: the initial spectrum of structure *2* was multiplied by 100.

diluted magnetic semiconductors are fairly low but can substantially exceed room temperatures in diluted ferromagnetic granulated alloys. It is therefore of interest to study supersaturated solid solutions of Mn in III–V semiconductors and, in particular, their galvanomagnetic properties.

The purpose of this work was to study the special features of the behavior of the Hall effect in Mn-supersaturated GaMnSb layers deposited by laser sputtering of undoped GaSb and metal Mn targets in a vacuum. It was found that acceptor-type defects were largely formed in the films prepared by laser plasma deposition. Moreover, the concentration of acceptor defects and, accordingly, the concentration of holes *p* could easily be controlled by changing the temperature of the substrate, which allowed *p* to be varied from 10^{19} to 5×10^{20} cm^{-3}. As distinct from the earlier results, we observed a positive high-temperature anomalous Hall effect that exhibited hysteresis up to room temperatures in the layers under study. Anomalous Hall effect data processing according to Belov and Arrott [21] allowed us to determine the value of T_C^* that characterized spontaneous manifestation of the (in the absence of a magnetic field) anomalous Hall effect. The T_C^* reached 330 K at $p = 5 \times 10^{20}$ cm^{-3} and decreased as the concentration of holes lowered. Physical reasons for the observed anomalous Hall effect characteristics and for its absence in similar structures that had been studied earlier will be considered.

2. EXPERIMENTAL PROCEDURE

GaMnSb films were deposited using a pulsed yttrium aluminum garnet laser operating in the

Q-switching mode at 1.06 μm. We used a rotating combined target consisting of a plate of single crystalline undoped GaSb covered in part by a high-purity Mn metal. The trace of material vaporization with the laser was a circle, and the ratio between the lengths of the arcs of sputtered GaSb and Mn therefore determined the level of growing layer doping. The films were deposited on a plate of semi-insulating GaAs with the (100) orientation, and the substrate temperature T_s was varied from 200 to 440°C. The resulting films were 40–140 nm thick.

The structural characteristics and composition of the films were studied by X-ray diffraction on a DRON-4 instrument using the two-crystal scheme and Cu $K_{\alpha 1}$ radiation filtered with a Ge(400) monochromator, X-ray photoelectron spectroscopy on a MicroLab MK II unit (VG Scientific) using nonmonochromatized Al K_α radiation, and electron probe microanalysis on a GAMEBAX unit. The magnetization of the films was measured by a BHV-50 vibrating-coil magnetometer with a sensitivity no worse than 10^{-5} emu.

The samples for Hall effect measurements were prepared by photolithography, as mesostructures with the standard double cross form (the width and length of the conduction channel were $W = 0.5$ mm and $L = 4.5$ mm, respectively). Hall effect measurements in fields up to 1 T were performed using an automated unit by the method of digital filtration and signal accumulation. The voltage between the Hall (V_y) and potential (V_x) probes and current I_x that passed through the sample were synchronously recorded under constant voltage conditions at positive and negative magnetic field B values; the field was applied normally to the film surface (along the *z* axis). The measurement results were used to determine the resistance of the sample between the potential probes $R_{xx} = V_x/I_x$ and transverse resistance $R_{xy} = V_y/I_x$. Preliminary experiments showed that transverse resistance could exhibit hysteresis and the magnetic field dependence of longitudinal resistance was negligibly small (the magnetoresistance of the films under study did not exceed 0.1%). Considering possible hysteresis, the Hall resistance R_H was determined by subtracting the even signal component from R_{xy} (the even component appeared because of asymmetry in the arrangement of Hall probes); that is, $R_H = R_{xy} - (R_{xy}^+ + R_{xy}^-)/2$, where R_{xy}^+ and R_{xy}^- are the transverse resistance values corresponding to the positive and negative magnetic field directions obtained, for instance, in scanning over the field as it decreased in magnitude (from 1 to 0 T).

3. RESULTS AND DISCUSSION

The X-ray diffraction θ/2θ spectra of the GaSb/GaAs structures deposited at a 440°C substrate temperature are shown in Fig. 1. The spectrum of the structure with a GaSb layer undoped by Mn (curve *1*)

contains a substrate peak at $2\theta = 66.05°$ (the GaAs(400) reflection) and a layer peak at $60.74°$ (the GaSb(400) reflection). The Bragg angles of the 2θ peaks from the layer and substrate were refined in two stages. At the first stage, we refined the angle of crystal rotation with a broad slit in front of the detector (ω scan). At the second stage, the angle of detector rotation was determined with a narrow slit while the sample rotation angle was fixed at a value corresponding to maximum intensity (θ scan). The substrate was used as a reference to correct the 2θ angle of the layer.

Calculations of the lattice parameter of undoped GaSb from the 2θ angle gave $a_0 = 0.6096$ nm, which coincided with the value known from the literature [19]. The integral characteristic of the structural perfection of the layer was the rocking curve width (full width at half maximum, FWHM) measured from the ω-scan spectrum according to [22]. The FWHM value for the peak from the GaSb layer was $\Delta\omega \approx 0.4°$. It follows that GaSb is a mosaic single crystalline film, although the fairly large $\Delta\omega$ value may be evidence of nonideality of the crystal structure of the film likely caused by the difference in the lattice constants of GaSb and GaAs exceeding 7%.

The X-ray diffraction $\theta/2\theta$ spectrum of the structure with a GaMnSb layer also deposited at 440°C is shown by curve 2 in Fig. 1. This spectrum is similar to that of GaSb free of Mn (curve 1). It follows that the introduction of Mn by laser plasma deposition does not cause noticeable structural imperfection of the deposited layers. With GaMnSb, the procedure for refining the Bragg angle of the 2θ peak GaSb(400) with the use of ω and θ scans, however, gives a value of $2\theta = 60.76°$, which is somewhat larger than that of the undoped layer. We used the equation $a(x) = a_0 - 0.00528x$, where a_0 is the lattice constant of undoped GaSb, for the lattice parameter of $Ga_{1-x}Mn_xSb$ with a zinc blende structure [23] and the $2\theta = 60.76°$ value obtained for GaMnSb layers grown at $T_s = 350–440°C$ to estimate the content of Mn, $x \approx 0.04 \pm 0.01$.

The FWHM value monotonically increases from $0.4°$ at $T_s = 440°C$ to $0.5°$ at $T_s = 300°C$ as the temperature of GaMnSb layer growth lowers. The GaSb(400) peak, although low-intensity, is observed even at $T_s = 200°C$. This is evidence that the presence of manganese in a layer of gallium antimonide in the concentration specified above has no substantial influence on the character of its growth during laser plasma deposition over the temperature range 200–440°C.

The composition of the films was studied by electron-probe microanalysis with a spatial resolution of order 1 μm. The results showed that Mn was fairly uniformly distributed over the area of the samples (the spread of x values was about 1%). The thickness of the films was much less than the region of X-ray radiation excitation by accelerated electrons in the structure, which prevented exact calculations of manganese contents from the data obtained this way. Estimates, however, show that the content of Mn in GaSb films was $x \approx 0.10$. This is larger than the value obtained from X-ray diffraction. This discrepancy can arise because electron-probe microanalysis measurements determine the chemical composition of the films, whereas X-ray diffraction is sensitive to changes in the GaSb lattice parameter caused by the insertion of Mn ions into gallium sublattice sites. When a nonequilibrium method for depositing layers is used, manganese atoms can enter into other lattice sites (for instance, into interstices) and form clusters. It follows that the $x \approx 0.10$ value is more realistic.

The suggestion of the possible presence of clusters is substantiated by the X-ray photoelectron spectra of the samples. The X-ray photoelectron spectra of GaMnSb/GaAs structures are presented in Fig. 2. The Mn $2p$ line spectrum is shown in Fig. 2a. This line has a complex structure, in which at least two chemical states of manganese atoms are distinctly seen. The positions of the Mn $2p_{3/2}$ peaks for these two states are denoted by A and B in the figure. The actual positions of peaks in the spectra of compounds is determined by several factors, in particular, by changes in the energy levels caused by chemical interaction (the so-called chemical shift [24]) and exchange interaction [25] in magnetic materials. The experimental (Fig. 2a) E_B values for the Mn $2p_{3/2}$ line in states A and B are 638.9 and 640.8 eV, respectively. The first value coincides with E_B for Mn metal (638.9 eV [26]). A similar splitting of the Mn $2p_{3/2}$ peak was observed in [25] for ternary alloys containing Mn and Sb. The first peak in [25] coincided with the manganese metal peak. The second peak at larger E_B values was split off by approximately 2 eV in a situation close to that considered in this work. It appeared in compounds probably because of exchange interactions caused by the chemical state of manganese atoms in which they have a large local magnetic moment [25]. It follows that there are at least two states of Mn atoms in GaMnSb films, one characteristic of bonds between Mn and Sb atoms and the other similar to the state of Mn in Mn metal (Mn–Mn bonds). The conclusion can be drawn that the films under consideration are supersaturated solid solutions of Mn in GaSb that contain the GaSb matrix with 4% of Ga replaced by manganese and manganese-containing clusters, whose influence on the magnetic and galvanomagnetic properties of the layers is discussed below.

Another special feature of the GaMnSb films is their primordially p-type conduction, even in the absence of doping, in particular, with manganese. This is likely related to the formation of antisite Ga_{Sb} defects (Ga atoms in Sb sites) during film growth, which are shallow acceptors in GaSb [19]. Indeed, as follows from the X-ray photoelectron spectra of GaMnSb layers shown in Fig. 2b (Ga $3d$ and Sb $4d$ lines) and 2c (two Sb $3d$ lines) (spectra 2 and 3) in comparison with the corresponding X-ray photoelectron spectra of single crystalline undoped GaSb (Fig. 2, spectrum 1), the
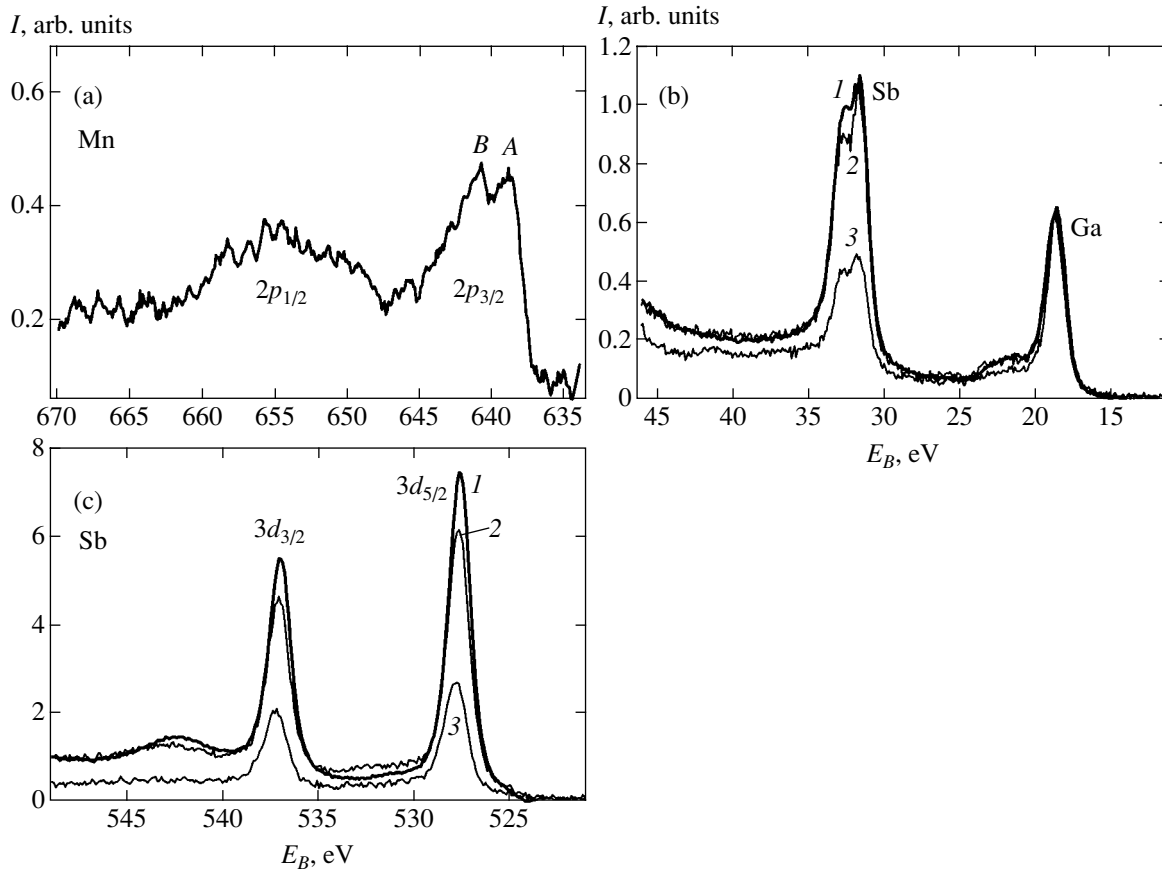
Fig. 2. X-ray photoelectron spectra: (a) Mn $2p$ line for a GaMnSb layer, $T_s = 200°C$; (b) Ga $3d$ and Sb $4d$ lines for (*1*) single crystalline GaSb, (*2*) a GaMnSb layer, $T_s = 440°C$, and (*3*) a GaMnSb layer, $T_s = 200°C$; and (c) Sb $3d$ lines for three types of structures, see (b).

content of Ga atoms in the films is higher than that of Sb atoms ($C_{Ga}/C_{Sb} > 1$). The nonstoichiometry of deposited layers (the C_{Ga}/C_{Sb} ratio) increases as the deposition temperature T_s decreases. According to the measurements performed at 300 K, the resistivity of the films ρ decreases from $\rho = 4 \times 10^{-2}$ Ω cm at $T_s = 440°C$ to $\rho = 3 \times 10^{-3}$ Ω cm at $T_s = 200°C$, which is evidence of an increase in the concentration of holes.

Measurements of the magnetization of the GaMnSb films grown at various temperatures gave the results shown in Fig. 3. We see that, in spite of the substantial differences in the conductivities of the layers deposited at various T_s (differences in hole concentrations), the films exhibit ferromagnetic behavior, and their saturation magnetizations do not vary strongly, from $M_s = 5.3$ mT at $T_s = 200°C$ to $M_s = 3.6$ mT at $T_s = 440°C$. We assume that the magnetic moment of the films is determined by Mn^{2+} ions [3] (g-factor = 2 and the total spin $S = 5/2$). On this assumption, calculations give Mn ion concentrations of $N_{Mn} = 1.1 \times 10^{21}$ cm^{-3} ($T_s = 200°C$) and $N_{Mn} = 7.8 \times 10^{20}$ cm^{-3} ($T_s = 440°C$), which is in agreement with maximum estimates of the concentration of Mn atoms as an impurity that replaces Ga, $N_{Mn} =$

7.1×10^{20}–1.8×10^{21} cm^{-3} at $x = 0.04$–0.10. However note that if the magnetic properties of III–Mn–V semiconductors weakly depend on the concentration of holes, they are usually related to the presence of MnSb- or MnAs-type ferromagnetic clusters [3, 8].
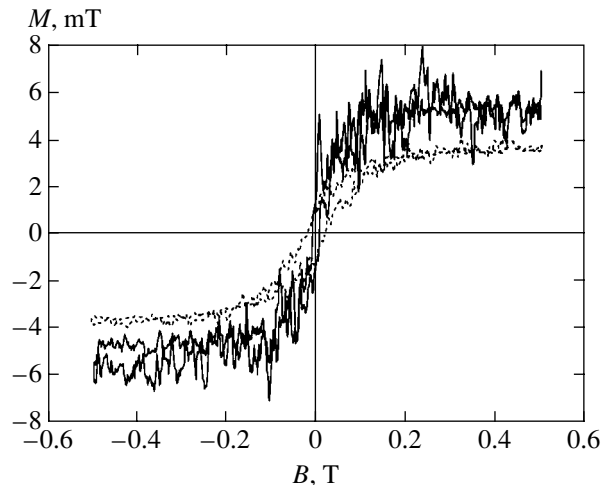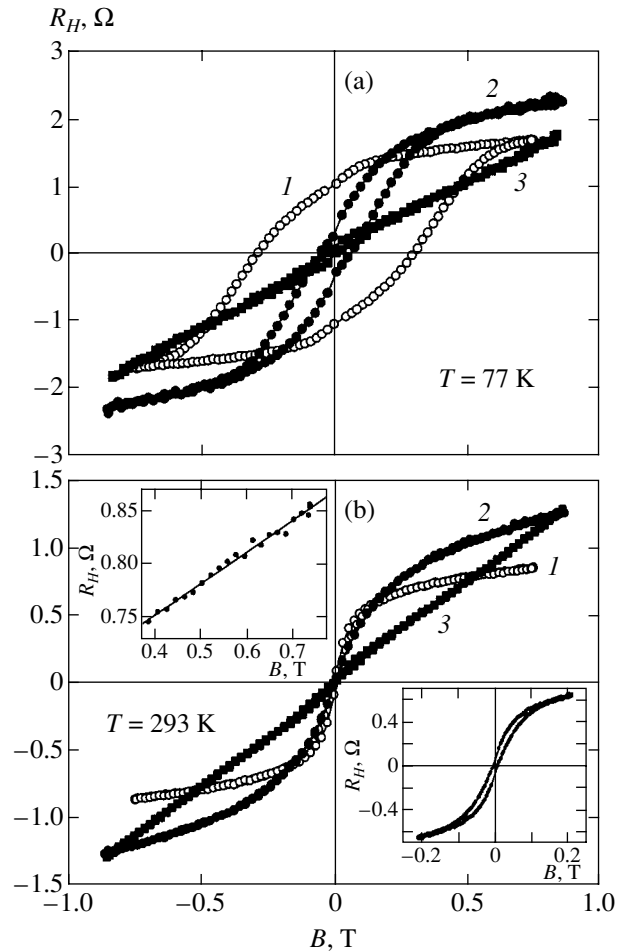

Fig. 3. Applied magnetic field dependences of magnetization for GaMnSb layers $d = 40$ nm thick, $T_s = 200°C$ (solid line), and $d = 140$ nm thick, $T_s = 440°C$ (dots).

As distinct from magnetization, the behavior of the Hall effect strongly depends on the concentration of holes (on the deposition temperature T_s). The magnetic field dependences of the Hall resistance $R_H(B)$ obtained at $T = 77$ and 293 K are shown in Figs. 4a and 4b, respectively, for samples 1–3 with hole concentrations $p = 5 \times 10^{20}$ cm^{-3} (curve 1), 1.5×10^{20} cm^{-3} (curve 2), and 3×10^{19} cm^{-3} (curve 3). The concentration of carriers was determined from the slope of the $R_H(B)$ dependence in fields $B > 0.4$–0.5 T. The linear character of this dependence for sample 1 over the specified field range is illustrated by the upper inset to Fig. 4b. On the whole, it follows from Fig. 4 that the Hall effect in samples 1 and 2 is essentially anomalous in character over the temperature range $T = 77$–300 K, whereas the Hall effect in sample 3 with the lowest concentration of holes ($T_s = 440$°C) is ordinary. Indeed, the Hall resistance of this sample linearly depends on B over the field range 0–0.9 T, although its magnetization reaches saturation already at $B > 0.2$ T (Fig. 3). A comparison of the data on samples 1 and 2 presented in Fig. 4 shows that the hysteresis character of the behavior of the anomalous Hall effect also becomes suppressed as the concentration of holes decreases. For instance, for sample 1 ($p = 5 \times 10^{20}$ cm^{-3}), the coercive field reaches $B_c = 0.29$ T at $T = 77$ K and the anomalous Hall effect hysteresis manifests itself up to room temperature ($B_c = 6.5$ mT, see the lower inset to Fig. 4b). At the same time, for sample 2 ($p = 1.5 \times 10^{20}$ cm^{-3}), $B_c = 0.058$ T at $T = 77$ K and no anomalous Hall effect hysteresis is observed at $T = 300$ K.

As the Hall resistivity is proportional to magnetization M when the anomalous Hall effect predominates (see (1)), it was suggested in [3, 15] that the procedure developed by Belov and Arrott [21] (the construction of the dependence of M^2 on B/M) can be used to determine the spontaneous Hall resistance R_H^s, which is proportional to the spontaneous magnetization M_s characteristic of ferromagnetic system ordering. According to [21], we must construct the dependence of R_H^2 on B/R_H and extrapolate its linear portion to the intersection with the axis of ordinates to determine R_H^s for our systems.

Examples of the dependences of R_H^2 on B/R_H for sample 1 at several measurement temperatures are shown in Fig. 5. At 267 and 293 K, the linear extrapolation of R_H^2 to $B = 0$ gives $(R_H^s)^2 > 0$, whereas linear extrapolation at $T = 335$ K gives a negative $(R_H^s)^2$ value, which means that there is no ferromagnetic ordering at this temperature. The temperature dependences of the spontaneous Hall resistance R_H^s obtained using the pro-

Fig. 4. Applied magnetic field dependences of Hall resistance for three GaMnSb/GaAs structure samples: (1) $p = 5 \times 10^{20}$ cm^{-3}, $T_s = 200$°C, $d = 40$ nm; (2) $p = 1.5 \times 10^{20}$ cm^{-3}, $T_s = 200$°C, $d = 70$ nm; and (3) $p = 3 \times 10^{19}$ cm^{-3}, $T_s = 440$°C, $d = 140$ nm. Curve numbers correspond to sample numbers. Measurement temperatures: (a) 77 K and (b) 293 K. The upper inset to Fig. 4b contains the $R_H(B)$ dependence for sample 1 at $B > 0.4$ T, and the lower inset, the $R_H(B)$ dependence for sample 1 at $-0.2 < B < 0.2$ T.

cedure suggested in [21] and the coercive field B_c are shown in Fig. 6 for sample 1. These results are evidence that the spontaneous Hall resistance in this sample persists up to the temperature $T_C^* \approx 330$ K.

The T_C^* parameter of single-phase III–Mn–V materials coincides with the Curie temperature T_C [3, 6]. This value can be determined by analyzing the behavior of the anomalous Hall effect in the paramagnetic temperature region [3, 14]. Indeed, the anomalous Hall effect constant is $R_s = cR_{xx}$ [12], where c is a temperature-independent coefficient, if the anomalous Hall effect is determined by the mechanism of skew scattering of carriers. For this reason, the ratio between the Hall R_H and longitudinal resistance R_{xx} is, according
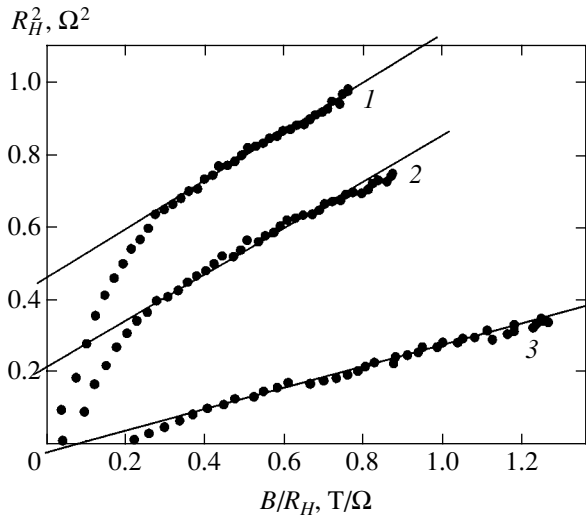
Fig. 5. Dependence of R_H^2 on B/R_H for sample 1 ($p = 5 \times 10^{20}$ cm^{-3}). Measurement temperatures (*1*) 267, (*2*) 293, and (*3*) 335 K.

to (1), $R_H/R_{xx} \approx cM/d$. It follows that, in the paramagnetic region, the magnetic susceptibility is

$$\chi \propto [d(R_H/R_{xx})/dB]_{B=0},$$

and the Curie–Weiss law $(1/\chi) \propto (T - T_C)$ can be used to determine T_C. It was shown in [3] for the example of GaMnAs that this approach gave the same T_C value as that obtained by analyzing the anomalous Hall effect in the ferromagnetic region.
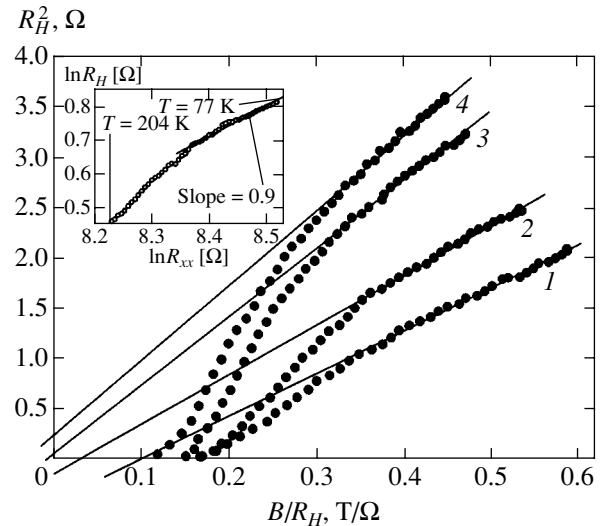
The Arrott dependences for sample 2 ($p = 1.5 \times 10^{20}$ cm^{-3}) over the range of temperatures $T \geq 160$ K are
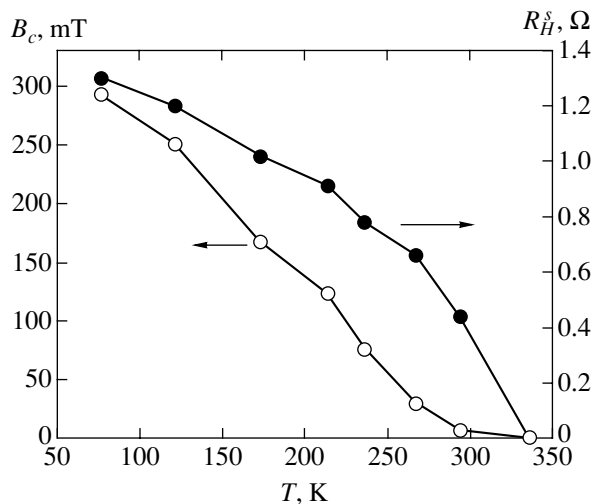
shown in Fig. 7. The linear extrapolation of these dependences gives their intersection with the origin at $T \approx 180$ K; that is, we can expect, by analogy with single-phase diluted magnetic semiconductors, that the Curie temperature of this sample is $T_C \approx 180$ K, and, starting with this temperature, the sample turns paramagnetic. The dependence of the Hall resistance on the longitudinal resistance obtained at $B = 0.75$ T is shown in the inset to Fig. 7 in the double logarithmic coordinates. The R_{xx} resistance of this sample increases as the temperature lowers. It follows from the data given in the inset to Fig. 7 that the slope of the dependence of $\ln R_H$ on $\ln R_{xx}$ in the region of low temperatures, where magnetization should weakly depend on T, is close to one; that is, the suggestion of the predominant role played by the mechanism of skew scattering of carriers in the anomalous Hall effect is justified for our systems. Seemingly, the slope of the dependence of R_H/R_{xx} on B in low fields, which is proportional to χ, should then increase as the temperature lowers. However, in reality, this slope is virtually independent of the temperature (see Fig. 8), which distinguishes our systems from single-phase diluted magnetic semiconductors of the GaMnAs type [3] (see the data presented in Fig. 3 and borrowed from [3]).

More substantial differences become evident when the special features of the anomalous Hall effect described above are compared with an analogous effect in GaMnSb layers prepared by molecular beam epitaxy at various growth temperatures [8]. It was found in [8] that Mn is almost fully contained in ferromagnetic MnSb clusters in layers grown at high temperatures of $T_s = 560°$C. The concentration of holes in the GaSb matrix is then 2.4×10^{19} cm^{-3} (in the sample with the

Fig. 6. Measurement temperature dependences of the coercive force of magnetization B_c (the left curve) and spontaneous Hall resistance component R_H^s (the right curve) for sample 1.


Fig. 7. Dependence of R_H^2 on B/R_H for sample 2 ($p = 1.5 \times 10^{20}$ cm^{-3}). Measurement temperatures (*1*) 254, (*2*) 226, (*3*) 180, and (*4*) 160 K; the relation between R_H and R_{xx} is shown in the inset to the double logarithmic coordinates.

total content of Mn $x = 0.013$), and the ordinary component predominates in the Hall effect to $T \approx 10$ K. In our systems, the Hall effect is only ordinary in sample 3 with a similar hole concentration ($p = 3 \times 10^{19}$ cm^{-3}), which is substantially lower than that in samples 1 and 2. The layers obtained in [8] at $T_s = 250°$C had the structure of zinc blende, in which Mn atoms largely replace Ga and play the role of acceptors. A well-defined negative anomalous Hall effect was then observed at low measurement temperatures (its sign was opposite to that of the ordinary Hall effect). The Belov–Arrott procedure was used in [8] to obtain $T_C^* \approx 25$ K at the hole concentration $p = 1.3 \times 10^{20}$ cm^{-3} (for the sample with the content of Mn $x = 0.016$). At the same time, sample 2 with approximately the same concentration of holes ($p = 1.5 \times 10^{20}$ cm^{-3}) had $T_C^* \approx 180$ K, and its anomalous Hall effect was positive.

Let us discuss the experimental data presented above. Note that, as in the samples studied in this work, the sign of the anomalous Hall effect in continuous MnSb films was positive [27]. It is reasonable to suggest that the sign of the anomalous Hall effect remains unchanged in passing from continuous to broken films. Indeed, we recently showed for the example of Fe nanoparticles in a SiO$_2$ matrix (the sign of the anomalous Hall effect in Fe was also positive) that the sign of the anomalous Hall effect did not change in the passage through the percolation threshold to tunnel conduction conditions [28]. The invariability of the sign of the anomalous Hall effect follows from the effective medium model [29]. Note also that, at the growth temperatures used ($T_s = 200$–$440°$C), the films contained a ferromagnetic phase in approximately equal concentrations (see the magnetization data given in Fig. 3).

The observations described above lead us to conclude that the anomalous Hall effect in the GaMnSb samples is related to the presence of MnSb-type clusters in them. The volume content of the ferromagnetic phase recalculated to MnSb ($M_s = 71$ mT [6]) is about 0.07, which is far below the critical value (0.6 [28]) corresponding to the metal–insulator percolation transition. The cardinal difference between our objects (the predominance of the anomalous Hall effect at fairly high temperatures) and samples with MnSb clusters [8] is the much higher concentration of holes in the GaSb matrix, which is related to the generation of acceptor-type defects (antisite Ga$_{Sb}$ defects) during film growth by the laser plasma deposition method. This is in agreement with the observed strong dependence of the behavior of the anomalous Hall effect on the concentration of carriers at a constant ferromagnetic phase concentration (see Fig. 4). We can therefore naturally suggest that the interaction of carriers with ferromagnetic clusters in semiconductors with magnetic impurities is to a considerable extent determined by the presence of Schottky barriers at the boundary between the clusters and the semiconducting matrix (in our system, at the
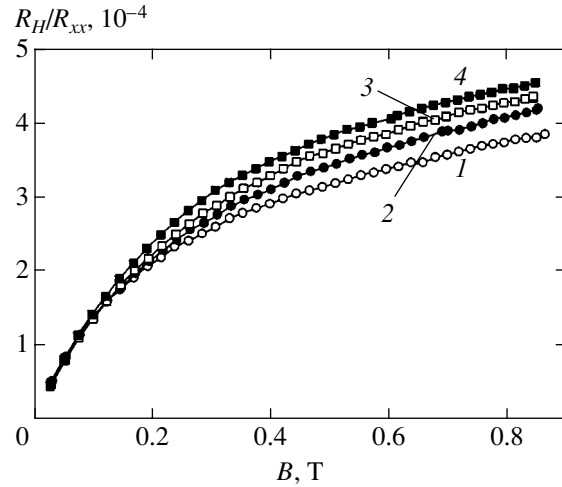
Fig. 8. Applied magnetic field dependences of the R_H/R_{xx} ratio for sample 2 at various measurement temperatures: (*1*) 293, (*2*) 254, (*3*) 226, and (*4*) 180 K.

MnSb/GaSb boundary). Accordingly, this interaction depends not only on the content of the ferromagnetic phase but also on the concentration of holes, whose increase decreases the width of the Schottky barriers. Estimates show that the expected Schottky barrier width must be about 2 nm at an $N_A^- \approx p = 10^{20}$ cm^{-3} concentration of ionized acceptors. This estimate was obtained on the assumption that the height of the Schottky barriers φ was determined by the position of the maximum of the density of surface states in the forbidden band of GaSb. In the majority of covalent semiconductors, this maximum is shifted from the valence band edge by one-third of the forbidden bandwidth E_g [30] ($E_g = 0.7$ eV for GaSb [19]). At the same time, for these conditions, the effective depth l_ψ of a decrease in the wavefunction of heavy holes ($m_{hh} = 0.23m_0$) under the barrier can be estimated at 1.3–2.5 nm; that is, it can even be larger than the Schottky barrier width at $p = 10^{20}$ cm^{-3} and $\varphi = (1/3)E_g$. We can then naturally expect strong tunnel exchange between matrix carriers and ferromagnetic clusters.[3] (The estimates for l_ψ were obtained using the equation for the transparency of a triangular barrier [30]; the lower estimate corresponds to the mean electric field in the region of the spatial charge of the Schottky layer, and the upper, to the maximum field.)

The temperature at which there is no anomalous Hall effect hysteresis is interpreted as the blocking temperature of ferromagnetic granulated alloys [20]; at this temperature, the transition to the superparamagnetic

---

[3] Note that the mean distance between ionized acceptors at $p = 10^{20}$ cm^{-3} is also about 2 nm. This leads us to conclude that the above estimates are actually evidence of the absence of Schottky barriers. The origin of the anomalous Hall effect is then similar to that in magnetic granulated alloys [20].

limit occurs. Estimates show that MnSb clusters of size $a_c \approx 10$ nm give blocking temperatures of order 200–300 K observed as Curie temperatures in our experiments (the estimates were obtained only taking into account the magnetic anisotropy energy related to the shape of the clusters [31]). Also note that the spread of the clusters in shape and size substantially weakens the temperature dependence of magnetization [32], which probably explains the absence of temperature effects on the paramagnetic behavior of the anomalous Hall effect in low fields (the weak dependence $\chi(T) \propto [d(R_H/R_{xx})/dB]_{B=0}$) observed for sample 2 (Fig. 8).

At the same time, it should be noted that the interpretation of the data on the anomalous Hall effect in terms of isolated (noninteracting) MnSb clusters and blocking temperatures encounters obvious difficulties. Indeed, an increase in the growth temperature T_s accompanied by a decrease in the concentration of holes should cause the enlargement of clusters. The high coercive force values observed experimentally are evidence that the clusters are single-domain; the coercive field is then the higher the larger the size of the clusters [33]. For this reason, increasing T_s should make the hysteresis character of the behavior of the anomalous Hall effect more manifest, which has not been observed experimentally, although the contribution of the ordinary component to the Hall effect increases because of a decrease in the concentration of current carriers. This leads us to suggest that the size of MnSb clusters (and, accordingly, the distance between them) is noticeably smaller than 10 nm and that these clusters interact with each other. This interaction is mediated by carriers in the paramagnetic GaSb:Mn matrix. This results in an effective enlargement of the clusters and, simultaneously, increases hole spin polarization, which determines the anomalous Hall effect.

4. CONCLUSIONS

To summarize, we prepared epitaxial films of a supersaturated solid solution of Mn in GaSb by laser plasma deposition. The special feature of the layers grown was the presence of dissolved Mn atoms and ferromagnetic Mn-containing inclusions. The layers also contained acceptor-type defects controlled by the growth temperature. These defects to a substantial extent determined the concentration of holes in the GaSb matrix, which increased as the growth temperature lowered and reached 5×10^{20} cm^{-3} at $T_s = 200$°C. Unlike single-phase GaMnSb systems, the films exhibited a positive anomalous Hall effect. Its hysteresis character strongly depended on the concentration of holes and could be observed up to room temperatures.

We believe that the special features of the behavior of the anomalous Hall effect in our systems are related to the interaction of charge carriers with ferromagnetic clusters, determined to a significant extent by the presence of Schottky barriers at the boundaries between the clusters and the semiconducting matrix. The role played by these barriers becomes less important as the concentration of holes increases. It can be thought that the enigmatic absence of the anomalous Hall effect in diluted magnetic semiconductors with ferromagnetic inclusions (MnSb or MnAs clusters with high Curie temperatures) discussed in the literature is most likely related to the presence of Schottky barriers at the boundaries between the clusters and semiconducting matrices. At low carrier concentrations (10^{19} cm^{-3}), the Schottky barriers are fairly wide and prevent the interaction of carriers with the ferromagnetic clusters.

Further studies are, however, necessary to elucidate the nature of ferromagnetic inclusions in the synthesized layers and the mechanism of their interaction mediated by the semiconducting matrix, which contains free carriers and magnetic ions in considerable concentrations. Such studies would certainly be of fundamental interest, especially in light of the recently discovered long-range character of exchange interactions between thin ferromagnetic layers through a semiconducting spacer [34].

REFERENCES

1. C. Timm, J. Phys.: Condens. Matter **15**, R1865 (2003).
2. H. Ohno, Science **291**, 840 (2001).
3. H. Ohno and F. Matsukura, Solid State Commun. **117**, 179 (2001).
4. X. Chen, M. Na, M. Cheon, *et al.*, Appl. Phys. Lett. **81**, 511 (2002).
5. T. Dietl, H. Ohno, and F. Mutsukura, Phys. Rev. B **63**, 195 205 (2001).
6. K. W. Edmonds, P. Boguslavski, K. Y. Wang, *et al.*, Phys. Rev. Lett. **92**, 037 201 (2004).
7. P. M. Krstajie, F. M. Peeters, V. A. Ivanov, *et al.*, Phys. Rev. B **70**, 195 215 (2004).
8. E. Abe, F. Matsukura, H. Yasuda, *et al.*, Physica E (Amsterdam) **7**, 981 (2000); F. Matsukura, E. Abe, Y. Ohno, and H. Ohno, Appl. Surf. Sci. **159**–**160**, 265 (2000).
9. H. Luo, G. B. Kim, M. Cheon, *et al.*, Physica E (Amsterdam) **20**, 338 (2004).
10. P. Mahadevan and A. Zunger, Phys. Rev. B **68**, 075 202 (2003).

11. C. Kittel, *Introduction to Solid State Physics*, 5th ed. (Wiley, New York, 1976; Nauka, Moscow, 1978).

12. A. V. Vedyaev, A. B. Granovskiĭ, and O. A. Kotel'nikova, *Kinetic Phenomena in Disordered Ferromagnetic Alloys* (Mosk. Gos. Univ., Moscow, 1992) [in Russian].

13. T. Jungwirth, Q. Niu, and A. H. McDonald, Phys. Rev. Lett. **88**, 207208 (2002).

14. A. M. Nazmul, S. Sugahara, and M. Tanaka, Phys. Rev. B **67**, 241308R (2003).

15. F. Matsukura, D. Chiba, T. Omiya, *et al.*, Physica E (Amsterdam) **12**, 351 (2002).

16. T. Adhikari and S. Basu, J. Magn. Magn. Mater. **161**, 282 (1996).

17. K. W. Edmonds, R. P. Campion, K.-Y. Wang, *et al.*, J. Appl. Phys. **93**, 6787 (2003).

18. T. Dietl, F. Matsukura, H. Ohno, *et al.*, cond-mat/0306484.

19. P. S. Dutta, H. L. Bhat, and V. Kumar, J. Appl. Phys. **81**, 5821 (1997).

20. A. Gerber, A. Milner, M. Karpovsky, *et al.*, Phys. Rev. B **69**, 134422 (2004); J. Magn. Magn. Mater. **242–245**, 90 (2002).

21. K. P. Belov, *Magnetic Transitions* (Fizmatgiz, Moscow, 1959; Consultants Bureau, New York, 1961); A. Arrott, Phys. Rev. **108**, 1394 (1957).

22. D. K. Bowen and B. K. Tanner, *High Resolution X-Ray Diffractometry and Topography* (Taylor and Francis, London, 1998; Nauka, St. Petersburg, 2002).

23. S. Basu and T. Adhikari, J. Alloy Comp. **205**, 81 (1994).

24. D. Woodruff and T. Delchar, *Modern Techniques of Surface Science* (Cambridge Univ. Press, Cambridge, 1986; Mir, Moscow, 1989).

25. M. V. Yablonskikh, Yu. M. Yarmoshenko, E. G. Gerasimov, *et al.*, J. Magn. Magn. Mater. **256**, 396 (2003).

26. C. J. Powell, Appl. Surf. Sci. **89**, 141 (1995).

27. I. K. Kikoin, N. A. Babushkina, and T. N. Igosheva, Fiz. Met. Metalloved. **10**, 488 (1960).

28. B. A. Aronzon, D. Yu. Kovalev, A. N. Lagar'kov, *et al.*, Pis'ma Zh. Éksp. Teor. Fiz. **70**, 87 (1999) [JETP Lett. **70**, 90 (1999)].

29. A. B. Granovsky, A. V. Vedyaev, and F. Brouers, J. Magn. Magn. Mater. **136**, 229 (1994).

30. S. Sze, *Physics of Semiconductor Devices*, 2nd ed. (Wiley, New York, 1981; Mir, Moscow, 1984).

31. V. V. Ryl'kov, B. A. Aronzon, A. B. Davydov, *et al.*, Zh. Éksp. Teor. Fiz. **121**, 908 (2002) [JETP **94**, 779 (2002)].

32. E. Z. Meĭlikhov, Zh. Éksp. Teor. Fiz. **116**, 2182 (1999) [JETP **89**, 1184 (1999)].

33. Yu. I. Petrov, *Physics of Small Particles* (Nauka, Moscow, 1982) [in Russian].

34. P. Walser, M. Hunziker, T. Speck, *et al.*, Phys. Rev. B **60**, 4082 (1999); R. R. Gareev, D. E. Burgler, M. Buchmeier, *et al.*, Phys. Rev. Lett. **87**, 157202 (2001).

Translated by V. Sipachev